ELSEVIER

17 November 1995

Chemical Physics Letters 246 (1995) 139–144

CHEMICAL PHYSICS LETTERS

Photo-stationary state of UV pumped matrix isolated O_2

A.V. Danilychev, V.A. Apkarian

Department of Chemistry, University of California, Irvine, CA 92717, USA

Received 24 July 1995; in final form 5 September 1995

Abstract

The 193 nm excitation of O_2 in crystalline Ar and Kr leads to a photo-stationary state, whereby $\approx 50\%$ of the population is transferred from $O_2(X^3\Sigma_g^-)$ to $a(^1\Delta_g)$. A kinetic analysis yields absorption cross sections of $\approx 10^{-21}$ cm^2, from X and a states, and establishes the final states as $A'(^3\Delta_u)$ and the repulsive $^1\Pi$ surface, respectively. The $A' \leftarrow X$ transition is enhanced ≈ 3 orders of magnitude in the solid, by borrowing intensity from the $^3\Pi \leftarrow X$ transition. Only molecules isolated at defect sites, undergo permanent dissociation. Substitutionally isolated O_2 does not dissociate at excess energies $\leqslant 2.5$ eV.

1. Introduction

Various aspects of photodynamics of molecular oxygen isolated in solid matrices have been studied in some detail [1–14]. The bulk of these studies have concentrated on the electronic states that correlate with the $O(^3P) + O(^3P)$ asymptote, states that are relatively poorly coupled by radiative transitions. The first strongly allowed electronic transition of O_2 is the $B \leftarrow X$ Schumann–Runge band [15]. While absorption spectra of this transition have been recorded in matrices [1–4], despite a significant effort [5], no emission has been observed from matrix isolated $O_2(B)$ due to its efficient predissociation [16]. Given the fact that the $B(^3\Sigma_u^-) \rightarrow X(^3\Sigma_g^-)$ transition carries an oscillator strength of near unity [17,18], it could be expected that if prepared near the bottom of the potential, free-to-bound type emission could be observed from the dissociating state with some measurable quantum yield. Such an observation could in principle allow a detailed mapping of dissociation–recombination dynamics in the solid. This was in part the motivation of the work to be described here. Another motivation was the possibility of in situ photogeneration of atomic oxygen by photolysis of molecular oxygen – a scheme that could avoid contamination of the host by other photofragments. Finally, photochemistry of O_2 initiated by near UV excitation, due to discrete and continuum absorptions in the Schumann–Runge band [19] as well as the Herzberg continua [20,21], remains the subject of significant interest in trying to account for sources of odd oxygen in the atmosphere [22,23]. The present results shed some light on this subject, even though they may be more directly related to the heterogeneous photochemistry of O_2.

The 193 nm output of the ArF laser is a convenient source for excitation of O_2. At cryogenic temperatures, this radiation is not in exact resonance with any of the vibronic states of $O_2(B)$. Nevertheless, irradiation at 193 nm leads to emission from all of the states that arise as a result of cage induced recombination of two ground state $O(^3P)$ atoms [9]. This recombinant emission allows an assessment of

SSDI 0009-2614(95)01078-5

caging probabilities. We have previously reported and discussed the emission spectra of the $A' \rightarrow X$, $c \rightarrow a$, and $b \rightarrow X$ transitions which are observed by 193 nm excitation of O_2 isolated in crystalline Ar, Kr and Xe [12]. More recently the same photophysics was also observed for O_2 isolated in D_2 matrices [13]. The anomalous emission spectra that arise by 193 nm irradiation of O_2 isolated in crystalline Xe due to quenching of the A' state has also been presented by Okada et al. [10]. A closer inspection of the time evolution of fluorescence intensities in crystalline Ar and Kr solids reveals that a photostationary state develops between the triplet ground state and the first excited singlet states of O_2. We present this observation below, with an analysis of the kinetics, to make conclusions regarding the nature of the electronic transitions involved, their absorption strengths, and the efficiency of caging of O atoms in crystalline hosts, at various excitation energies.

2. Experimental

The experimental methods employed in the present work have been previously discussed in some detail [12]. They are carried out in free standing crystals of Ar and Kr, prepared from premixed samples containing O_2 at mole ratios of 1:1000 to 1:50000. A closed cycle He-refrigerator is used for crystal growth, affording a base temperature of ≈ 8 K in the crystal. The sample temperature is measured using a thermocouple embedded in the $1 \times 1 \times 1$ cm^3 crystal. An ArF laser (Lambda Physik, EMG 201) is used as an irradiation source, typically focusing pulses of 1–10 mJ on a 300×300 μm area, at repetition rates ranging from 1 to 10 Hz. The doubled output of an excimer pumped dye laser was used for survey scans of O_2 excitation spectra in the spectral range of 220–245 nm, while recording dispersed emission through a 0.25 m monochromator (McPherson 218).

3. Results

The key results of our focus are illustrated in Figs. 1 and 2. In Fig. 1a, the $A' \rightarrow X$ emission intensity of O_2 is shown as a function of irradiation time. The same data are shown in Fig. 1b, after normalization with the laser intensity. Several irradiation cycles at a constant laser repetition rate of 10 Hz are shown, with different dark periods between irradiation cycles. Several observations are to be noted in this sequence. Within a given irradiation cycle, the emission intensity is observed to decrease until a plateau is reached. The plateau level is proportional to the laser intensity, which is verified by the constancy of this level when the signal is normalized, as in Fig. 1b. The signal decay rate is proportional to the laser power. A decay rate of 6.7 ± 1 s is observed in the first cycle, which was obtained by focusing 10 mJ pulses on a 300×300 μm^2 area, at a repetition rate of 10 Hz. When the laser intensity is halved, so is the decay rate and the plateau level reached. Finally, the peak intensity at the beginning of a cycle is observed to be higher when preceded by a longer dark period. The recovery rate can be determined from a plot of peak intensity versus dark

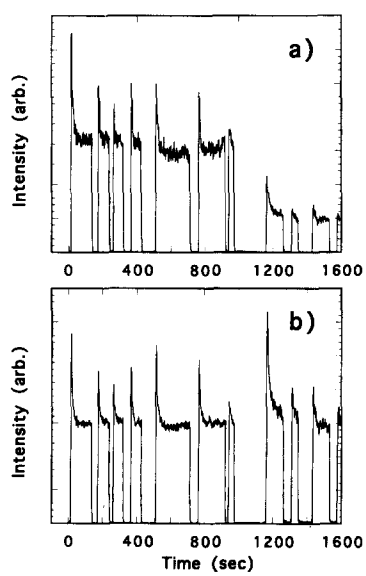

Fig. 1. $A' \rightarrow X$ emission intensity monitored as a function of time during a sequence of irradiation cycles, (a) raw data, (b) normalized to laser intensity. The signal decays during a particular exposure period to a plateau, and recovers when kept in the dark. The intensity of the laser was reduced by 60% after 1000 s, leading to a proportional decrease in the decay rate, and plateau level (a). The plateau level is constant when normalized (b). The data is from a free standing crystal of Ar containing 50 ppm $^{18-18}O_2$.

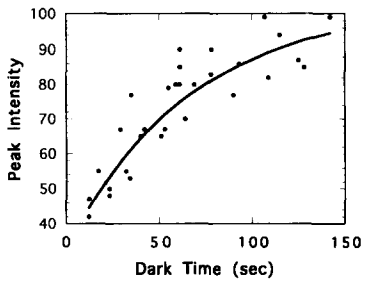

Fig. 2. Recovery of the A′ → X emission intensity as a function of dark time. An exponential fit to the data with a rise time of 67 s is shown along with the data.

time between irradiation cycles, which is shown in Fig. 2. The recovery rate extracted from the exponential fit, which is also shown in Fig. 2, is 70 ± 15 s.

The above observations are common to both Ar and Kr samples, and insensitive to isotopic composition of oxygen (^{18}O or ^{16}O). The analogous measurements were not pursued in Xe. In solid D_2, the signals are too week and a similar study could not be performed under our experimental conditions [13]. In all of these samples, upon 193 nm irradiation, O atoms could also be identified by their $^1S \rightarrow {}^1D$ emission which occurs in the spectral range 560–600 nm. A detailed analysis of these atomic emissions has already been given [12]. The presence of O atoms clearly implies permanent dissociation of O_2. However, this represents a very small ensemble of the molecules, such that the permanent bleach of the O_2 signal is not measurable within the signal-to-noise ratio of the experiments (less than 5% of the total O_2 concentration undergoes permanent dissociation). Moreover, successive annealing cycles completely eliminate the O atom signal, without any apparent effect on the reversible O_2 photophysics illustrated in Figs. 1 and 2. These observations lead us to conclude that permanent dissociation of O_2 occurs only at defect sites. We also establish that such defects can be annealed away in the free standing crystals. However, the nature of the defects remains unclear.

It is possible to directly establish that the reversible bleaching of the A′ → X emission is due to transfer of population to metastable states, as opposed to photodissociation and thermal recombination of atoms. This is achieved by observing resonances from the metastable states. The spectral range between 240 and 220 nm, which is above the dissociation limit of O_2 and a range where only continuum absorption is possible from $X(v = 0)$, was investigated by scanning a doubled dye laser while monitoring emission over $A'(v = 0) \rightarrow X(v = 8)$ transition. A congested spectrum, with sharp resonances above a continuous background was observed [24]. The appearance of discrete absorptions in this spectral range can only be attributed to transitions terminating in vibrationally excited states of $O_2(B)$, and therefore initiating from $O_2(X)$ near $v = 9$.

4. Discussion

The reversible bleaching of the fluorescence from $O_2(A')$ clearly indicates that the ground state population is being transferred to a metastable state which acts as a reservoir. The signal recovery time then must correspond to the lifetime of this state. The observed recovery time of 70 ± 15 s closely agrees with previous measurements of the lifetime of $a(^1\Delta_g)$, of 1 min, [9] (85 ± 10 and 72 ± 3 s in Ar and Kr matrices, respectively) [8]. The fact that a plateau, proportional to the irradiation intensity is reached, implies that a laser intensity independent equilibrium is reached between the populations of the X and a states. This in turn implies that a photo-stationary state is being developed, i.e. an equilibrium is reached between photo-induced population and photo-induced depopulation of the a state. Note that the time scale for establishment of the photo-stationary state and its recovery are many seconds. On this timescale the population of all excited states above $b(^1\Sigma_g^-)$ are negligible: the B state lifetime due to its predissociation is extremely short, $< 10^{-10}$ s, and the c, A′ and A states interconvert and decay by radiation on a timescale of < 100 ms [7–13]. Thus, it is safe to assume that the directly accessed states by 193 nm are completely depopulated on the multi-second timescales of the observed equilibrium. With these considerations in mind, the observed kinetics can be treated in the framework of a three level system. The ground state, as state 1; the reservoir state, which was already identified as $a(^1\Delta_g)$, as state 2; and the

optically accessed upper states, as state 3. The relevant kinetic equations are

$$\frac{dN_1}{dt} = -\sigma_{13} I N_1 + k_{21} N_2, \quad (1)$$

$$\frac{dN_2}{dt} = -\sigma_{23} I N_2 - k_{21} N_2 + k_{32} N_3,$$

$$\frac{dN_3}{dt} = \sigma_{13} I N_1 + \sigma_{23} I N_2 - k_{32} N_3,$$

where σ represents absorption cross sections in cm^2, I is the radiation flux in photons cm^{-2} s^{-1}, and k represent non-radiative relaxation rate constants that tie the various electronic states. On the many-seconds timescale, the steady-state approximation is clearly valid for the population in state 3, which also leads to the population conservation condition: $N_1(t) + N_2(t) \equiv 1$. The time dependent populations can then be obtained,

$$N_1 = \frac{\sigma_{13} I}{\sigma_{13} I + k_{21}} \left\{ \exp[-(\sigma_{13} I + k_{21}) t] + \frac{k_{21}}{\sigma_{13} I} \right\}, \quad (2)$$

such that at long time, $t = \infty$,

$$N_1^\infty = \frac{k_{21}}{\sigma_{13} I + k_{21}}, \quad \text{and } N_2^\infty = \frac{\sigma_{13} I}{\sigma_{13} I + k_{21}}. \quad (3)$$

Since the observed fluorescence signal intensity from the A′ state, $S(t)$, is directly proportional to the total optical pump rate. Assuming that the quantum yield of populating the A′ state is independent of the specific state reached by 193 nm excitation, the extent of the bleach can be expressed as

$$\frac{S(t=0)}{S(t=\infty)} = \frac{\sigma_{13} I}{\sigma_{13} I N_1^\infty + \sigma_{23} I N_2^\infty} = \frac{\sigma_{13} I + k_{21}}{\sigma_{23} I + k_{21}}. \quad (4)$$

Accordingly, a photo-stationary state can only be reached for irradiation intensities such that the optical pump rates are much greater than the decay rate of the reservoir state, $\sigma_{13} I$, $\sigma_{23} I \gg k_{21}$, leading to the observed intensity independent ratio,

$$\frac{S(t=0)}{S(t=\infty)} = \frac{\sigma_{13}}{\sigma_{23}}. \quad (5)$$

Under these conditions, the rate at which the stationary state is reached is simply given from Eq. (2) as $\sigma_{13} I$. Using the measured laser flux, $\sigma_{13} = 2(\pm 0.5) \times 10^{-21}$ cm^2 is determined. From Eq. (5) and the observed extent of bleach of $\approx 50\%$ σ_{23} is obtained as $\approx 1 \times 10^{-21}$ cm^2. The recovery rate is obtained from the equilibration rate of Eq. (2) by setting $I = 0$, yielding $k_{21} = 1/70$ s^{-1}.

While the above kinetic treatment is successful in accounting for the observed photophysics, its application should in principle be contingent upon establishing that the radiative relaxation of the a state is the rate determining step in the overall vibronic relaxation of matrix isolated O_2. However, it is known that this is not the case. While relaxation of all states above the b state proceed on time scales shorter than 100 μs, and the b state equilibrates with the a state via radiation on a time scale of 25 ms [9]; vibrational relaxation in $O_2(X)$ is extremely slow [14]. The $X(v = 6)$ state has a lifetime of 150 s in Ar, and the lower vibrational states relax on successively longer timescales, reaching a lifetime of 1650 s for $X(v = 1)$ [14]. The success of the simple kinetic model in analyzing the experimental data can only be rationalized if state 1 is identified with the electronic state X irrespective of its vibrational energy content. This could not be possible if the excitation were due to discrete vibronic resonances. The model then suggests that the final state is a continuum, accessible from a large range of vibrationally excited initial states. This conclusion is consistent with two other observations. It is known that the B state undergoes a significant matrix shift in its electronic origin, such that while in Ar 193 nm falls between $v = 3$ and 4 in Kr it falls between $v = 2$ and 3 of the B state [1,2]. Yet the observed results are virtually identical in Ar and Kr. Moreover, if the absorptions were due to discrete resonances then a strong isotopic dependence of cross sections would be expected. We have verified the absence of such an isotopic dependence, further establishing that the terminal state in the 193 absorption is a continuum. These arguments also apply for the 193 nm absorption from the a state, there too the absorption must terminate in a continuum.

It is quite informative to consider the possible origins of the observed absorptions. In all observed molecular transitions of O_2 in matrices, spin selec-

tion rules are well conserved. Therefore candidate continua for absorption from the $X(^3\Sigma_g^-)$ state are: the repulsive $1^3\Pi_u$ state, and the repulsive walls of $A'(^3\Delta_u)$ and $A(^3\Sigma_u^+)$ above their dissociation limits. While the $1^3\Pi_u$ potential, which crosses the inner turning point of the B state near $v = 2$ is in principle energetically accessible, Franck–Condon factors make this direct transition strictly prohibitive [25–27]. This cross section can be estimated to be significantly smaller than 10^{-25} cm^2 by extrapolating the calculated values of Allison et al. to 193 nm [27]. Thus, we are left with the Herzberg continua which at 193 nm have absorption cross sections of 1×10^{-24} and 7×10^{-24} cm^2, for the $A' \leftarrow X$ and $A \leftarrow X$ transitions, respectively [21]. In the bound region of the Herzberg states, A, A′ and c, although Franck–Condon factors are similar, the $A' \leftarrow X$ transition carries the intensity, and based on the observed radiative lifetime of the A′ state it has been well established that the A′–X transition is enhanced by ≈ 4 orders of magnitude [7,13]. Moreover, polarization measurements in matrices show that the A′–X transition dipole is perpendicular to the molecular axis, which has recently been argued to imply that this orbitally forbidden transition borrows intensity by mixing with the repulsive $^3\Pi$ state [13]. Thus, the 193 nm absorption from the X state can be uniquely ascribed to absorption to the repulsive wall of the A′ state, where Franck–Condon factors are optimal, and as in the bound region of the A′ state the oscillator strength of this transition in the matrices is enhanced by several orders of magnitude by mixing with the $^3\Pi$ state. As to the continuum absorption from the singlet states at 193 nm, consideration of both Franck–Condon and selection rules leads to the identification of the repulsive $^1\Pi$ state as the terminal state [25,26]. To our knowledge, the $^1\Pi \leftarrow a$ transition has not been characterized in the gas phase. The presently observed cross section of 10^{-21} cm^2 for this transition seems reasonable without invoking any special matrix effects.

Finally, we point out that under intense UV irradiation, a very efficient cage effect prevents O_2 from dissociation in crystalline Ar and Kr. Note, that where vibrationally excited states of the singlet manifold serve as the initial states in the excitation, the molecule is prepared at excitation energies of ≈ 2.5 eV above its dissociation limit. Yet, except for a very minor population of molecules isolated in defective sites, no permanent dissociation is observed.

5. Conclusions

We demonstrate that excitation of matrix isolated O_2 at 193 nm leads to efficient excitation of the molecule, whereby nearly 50% of the ground state population is transferred to the metastable singlet manifold. The near UV absorptions of O_2 arise from the Herzberg continuum, and the discrete and continuum absorptions of the Schumann–Runge band. While 193 nm falls in this spectral region, in cryogenic solids where only $v = 0$ in the ground state of the molecule is populated, due to poor Franck–Condon factors the Schumann–Runge band cannot contribute to the observed absorptions [26]. The observed absorption from the ground state is only consistent with the $A' \leftarrow X$ transition. The observed absorption cross section of $\approx 10^{-21}$ cm^2 is nearly three orders of magnitude larger than what is observed for the same transition in the free molecule [20,21]. This enhancement of the A′–X transition in matrices has already been noted, and has been uniquely ascribed to mixing between the $A'(^3\Delta_u)$ and $1^3\Pi_u$ states by polarization experiments [13]. The observation of the development of a photo-stationary state leads to the conclusion that an equally strong transition connects the $a(^1\Delta_g)$ state to a continuum, and the likely candidate for the latter is identified as $O_2(^1\Pi \leftarrow a)$. Finally, the absence of any permanent bleaching of the laser induced $A' \rightarrow X$ fluorescence, leads us to conclude that even at excess energies of ≈ 2.5 eV the lattice cage prevents the molecules from dissociation. Instead of dissociation, a photo-stationary state is reached between the triplet ground state and the singlet manifold of the molecule, until the latter relaxes by radiation on a timescale of 70 ± 15 s.

Acknowledgements

This research was supported under a grant from the US Air Force Office of Scientific Research: AFOSRF49620-1-0251.

References

[1] O. Schnepp and K. Dressler, J. Chem. Phys. 42 (1965) 2482.
[2] E. Boursey, J. Roncin and N. Damany, Chem. Phys. Letters 5 (1970) 584.
[3] I. Ya Fugol, L.G. Gimpelevich and L.I. Timchenko, Opt. i Spectroskopiya 40 (1976) 279.
[4] J. Bahrdt and N. Schwentner, J. Chem. Phys. 85 (1986) 6229.
[5] A. Salloum, H. Dubost and V.A. Apkarian, unpublished results.
[6] J.L. Richards and L. Johnson, J. Chem. Phys. 65 (1976) 3948.
[7] J. Goodman and L.E. Brus, J. Chem. Phys. 67 (1977) 1482; R. Rossetti and L.E. Brus, J. Chem. Phys. 71 (1979) 3963.
[8] K.P. Crone and K.J. Kügler, Chem. Phys. 99 (1985) 293.
[9] A.C. Becker, U. Schurath, H. Dubost and J.P. Galaup. Chem. Phys. 125 (1988) 321.
[10] F. Okada, H. Kajihara and S. Koda, Chem. Phys. Letters 192 (1992) 357.
[11] H. Kajihara, T. Okamura, F. Okada and S. Koda, Laser Chem. 15 (1995) 83.
[12] A.V. Danilychev and V.A. Apkarian, J. Chem. Phys. 99 (1993) 8617; J. Chem. Phys. 100 (1994)5556.
[13] A.V. Danilychev, V.E. Bondybey, V.A. Apkarian, S. Tanaka, H. Kajihara and S. Koda, J. Chem. Phys. (1995), in press.
[14] A. Salloum and H. Dubost, Chem. Phys. 189 (1994) 179.
[15] P. Krupenie, J. Phys. Ref. Data 1 (1972) 2.
[16] P.C. Cosby, H. Park, R.A. Copeland and T.G. Slanger, J. Chem. Phys. 98 (1993) 5117.
[17] D.C. Cartwright, N.A. Fiamengo, W. Williams and S. Trajmar, J. Phys. B 9 (1976) L419.
[18] A.C. Allison, S.L. Guberman and A. Dalgarno, J. Geophys. Res. 91 (1986) 10, 193.
[19] R.P. Saxon and T.G. Slanger, J. Geophys. Res. Atmos. 96 (1991) 17, 294.
[20] Z.C. Bao, W.O. Yu and J.R. Barker, J. Chem. Phys. 103 (1995) 6.
[21] R.P. Saxon and T.G. Slanger, J. Geophys. Res. Atmos. 91 (1986) 9877.
[22] T.G. Slanger, Science 265 (1994) 1817.
[23] R.L. Miller, A.G. Suits, P.L. Houston, R. Toumi, J.A. Mack and A.M. Wodtke, Science 265 (1994) 1831.
[24] A.V. Danilychev, Ph.D. Thesis (UC Irvine, 1994).
[25] P.S. Julienne, J. Mol. Spectry. 63 (1976) 60; P.S. Julienne and M. Krauss, J. Mol. Spectry. 56 (1975) 270.
[26] R.J. Buenker, S.D. Peyerimhoff and M. Peric, Chem. Phys. Letters 42 (1976) 383.
[27] A.C. Allison, S.L. Guberman and A. Dalgarno, J. Geophys. Res. 87 (1982) 923.